STM JOURNALS

Journal of
Polymer & Composites

ISSN: 2321-2810 (Online)
ISSN: 2321-8525 (Print)
Volume 13, Issue 3, 2025
DOI (Journal): 10.37591/JoPC

https://journals.stmjournals.com/JOPC/

Research JoPC

# Comparative Analysis of 3D-Printed and Molded Shape-Stabilized Phase Change Composites

Deepak Kumar Yadav[1,]*, Pushpendra Kumar Singh Rathore[2], Rajeev Kumar Singh[3], Arvind Kumar Gupta[4], Basant Singh Sikarwar[5]

***Abstract***

*Thermal energy storage (TES) has become essential for efficiently storing and utilizing thermal energy across applications like industrial heating, power plants, batteries, medical devices, food preservation, and aerospace technology. Because of their high energy density, affordability, and environmental friendliness, phase change materials, or PCMs, are employed extensively. However, challenges like poor thermal conductivity and leakage limit their performance. To address these issues, 3D printing has emerged as a powerful tool for developing PCM-based composites with improved thermal properties and structural stability. By enabling precise control over material composition, 3D printing enhances thermal conductivity and minimizes leakage, making TES systems more efficient and reliable. Latent heat storage (LHS) systems, in particular, benefit from 3D-printed PCM materials, offering a promising solution for energy efficiency and sustainability. In this work, the fused filament fabrication (FFF) technique was employed to create shape-stabilized composite phase change materials (SSPCMs). Initially, filaments were produced using a filament extruder with a composition of high-density polyethylene (HDPE), soy wax, paraffin wax, and nano-additives. These filaments were then used in a fused deposition modeling (FDM) 3D printer to fabricate SSPCM samples with 3% percentage of nano-additives, specifically Carbon-based nanomaterials, including multi-walled nanotubes (MWCNT) and graphene nanoplatelets. The thermal conductivity of these 3D-printed samples was compared with that of traditionally prepared SSPCM samples to evaluate the improvement achieved through additive manufacturing.*

**Keywords:** Thermal energy storage, phase-change materials, 3d printing, nanomaterials and latent heat storage

***Author for Correspondence**
Deepak Kumar Yadav
E-mail: yadav.deepak944@gmail.com

[1]Research Scholar, Department of Mechanical Engineering, Amity University, Noida, Uttar Pradesh, India
[2]Associate Professor, Department of Mechanical Engineering, Amity University, Noida, Uttar Pradesh, India
[3]Associate Professor, Department of Mechanical Engineering, Amity University, Noida, Uttar Pradesh, India
[4]Professor, Department of Mechanical Engineering, J.C. Bose University of Science and Technology, YMCA, Faridabad, Haryana, India
[5]Professor, Department of Mechanical Engineering, Amity University, Noida, Uttar Pradesh, India

Received Date: April 09, 2025
Accepted Date: April 17, 2025
Published Date: May 15, 2025

**Citation:** Deepak Kumar Yadav, Pushpendra Kumar Singh Rathore, Rajeev Kumar Singh, Arvind Kumar Gupta, Basant Singh Sikarwar. Comparative Analysis of 3D-Printed and Molded Shape-Stabilized Phase Change Composites. Journal of Polymer & Composites. 2025; 13 (3): 184–192p.

## INTRODUCTION

The energy storage capacity (KWh) and heat transfer rate (KW) of a phase change material (PCM) device influence its efficiency. While many PCMs have high energy storage potential, their low thermal conductivity can slow heat transfer, making it challenging to distribute heat through big slabs of PCM. Two approaches have been investigated by researchers to overcome this: (a) increasing thermal conductivity by adding materials such as expanded graphite, carbon fibers, or metallic particles; and (b) more efficiently distributing heat by employing metal fin structures or metallic foams [1-3]. However, these additions can reduce the overall PCM volume, impacting storage capacity. A Ragone plot, commonly used for battery performance analysis, is also useful for evaluating thermal energy storage (TES) heat exchangers [4-5]. It helps assess the trade-off between energy storage and power output. Increasing thermal conductivity reduces heat resistance and enhances power density, but it may also decrease the available storage capacity [6-8]. The ideal balance between energy and power depends on the application; for example, building insulation requires slow energy release over hours, while electronics cooling demands rapid heat dissipation within minutes [9-10]. Additive manufacturing (AM) plays a crucial role in improving TES heat exchangers by enabling complex designs that enhance heat transfer. Additive manufacturing (AM) allows the design of lightweight, high-efficiency heat exchangers with increased surface-area-to-volume ratios, optimizing PCM storage and heat transfer [11-13]. Advances in 3D printing now allow direct integration of PCM into structural materials through methods like blending, particle dispersion, and coaxial extrusion. PCMs used in AM are mostly organic because of their high latent heat, low corrosivity, and thermal stability. Common PCMs include paraffin's, alkenes, polyethylene glycols (PEGs), sugar alcohols, fatty acids, and water. Metal-based PCMs, such as nickel-titanium alloys and aluminum-tin composites, have also been explored for their unique phase transition properties. Specialized PCMs, such as stearyl acrylates, have been developed for chemical modifications and polymerization. Filament-based AM is widely used due to its affordability, minimal post-processing, and material versatility [14-15]. However, it has limitations such as lower resolution, weak layer adhesion, and the need for support structures. PCM integration in filaments is done through neat PCM blending, microencapsulation, or copolymerization. Polymers such as high-density polyethylene (HDPE), Acrylonitrile-butadiene-styrene (ABS), thermoplastic polyurethane (TPU), polycaprolactone (PCL), and nylon are commonly used. For direct PCM incorporation, the PCM must remain within the filament during extrusion and printing. This has been achieved through solution-phase mixing with PCL and melt-state blending with HDPE [17-18]. For instance, HDPE-based filaments with 40% PCM exhibited good extrusion properties and stored 64 J/g of energy. PCL filaments could hold up to 60% PCM, However, after printing, the energy storage decreased from 25 J/g to 10 J/g because only 20% of PCM filaments were effectively printed. These findings highlight the challenges and advancements in PCM-based AM for efficient thermal energy storage [19-20].

## MATERIAL & METHODS

High-density polyethylene (HDPE) granules, possessing a melt flow rate of 20 g/10 min and a specific gravity of 0.955 (tested at 190°C under a 2.16 kg load), were sourced from GAIL (India) Ltd. Both paraffin wax and soy wax were utilized in the study had a purity of over 95%, were obtained from Sigma-Aldrich, USA. Multi-Walled Carbon Nanotubes (MWCNT) had a density of 0.03 g/cm³, a thermal conductivity of more than 3000-3100 W/m-K, an average diameter of 8.7-10 nm, and a purity of above 98%. With an average diameter of 1–5 nm, a density of 0.014 g/cm³, a purity of over 99.9%, and a thermal conductivity of over 4000 W/m-K, graphene nano powder was impressive. Table 1 shows the material composition (HDPE, soy wax, paraffin wax, MWCNT, GNP) for four SSCPCM sample types.

### Preparation of Extruded Filament

Using a single screw extruder, composite filaments were prepared by combining HDPE, soy wax or paraffin wax, and either MWCNT or GNP. The mixture contained 40% paraffin wax and 35% soy wax by weight. The PCM/HDPE mixture was wrapped into a shredder and then extruded into composite filaments using a filament extruder. The extruder featured a single screw to enhance mixing and was equipped with four independent heating elements, each set to different temperatures. The extrusion process required a careful balance between material temperature and flow through the nozzle. A screw speed of 3 to 6 rpm was maintained, with heater temperatures ranging from 170°C to 210°C to ensure proper melting and smooth material movement [16]. Figure 1 illustrates the layout of the extrusion system used to create composite filaments for printing.

**Table 1.** Sample composition for SSCPCM

| Sample | HDPE | Soy wax | Paraffin wax | MWCNT | GNP |
|---|---|---|---|---|---|
| HDPE/PW/MWCNT3 | 60 | - | 37 | 3 | - |
| HDPE/PW/GNP3 | 60 | - | 37 | - | 3 |
| HDPE/SW/MWCNT3 | 65 | 32 | - | 3 | - |
| HDPE/SW/GNP3 | 65 | 32 | - | - | 3 |

 

Journal of Polymer & Composites
Volume 13, Issue 3
ISSN: 2321-2810 (Online), ISSN: 2321-8525 (Print)

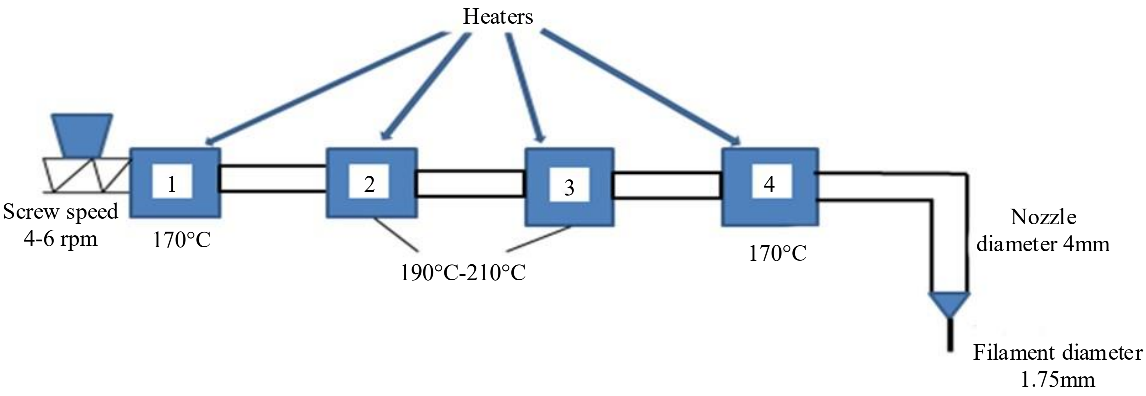


**Figure 1.** Systematic diagram of filament extruder.

**Table 2.** 3D Printer Settings.

| Setting | Value |
|---|---|
| Nozzle Diameter | 0.35mm |
| Nozzle temperature | 240ºC |
| Height of 1 layer | 0.20mm |
| Line Width | 0.40mm |
| Temperature of Build Plate | 60ºC |
| Fill Percentage | 100% |
| Printing Speed | 1100mm/min |

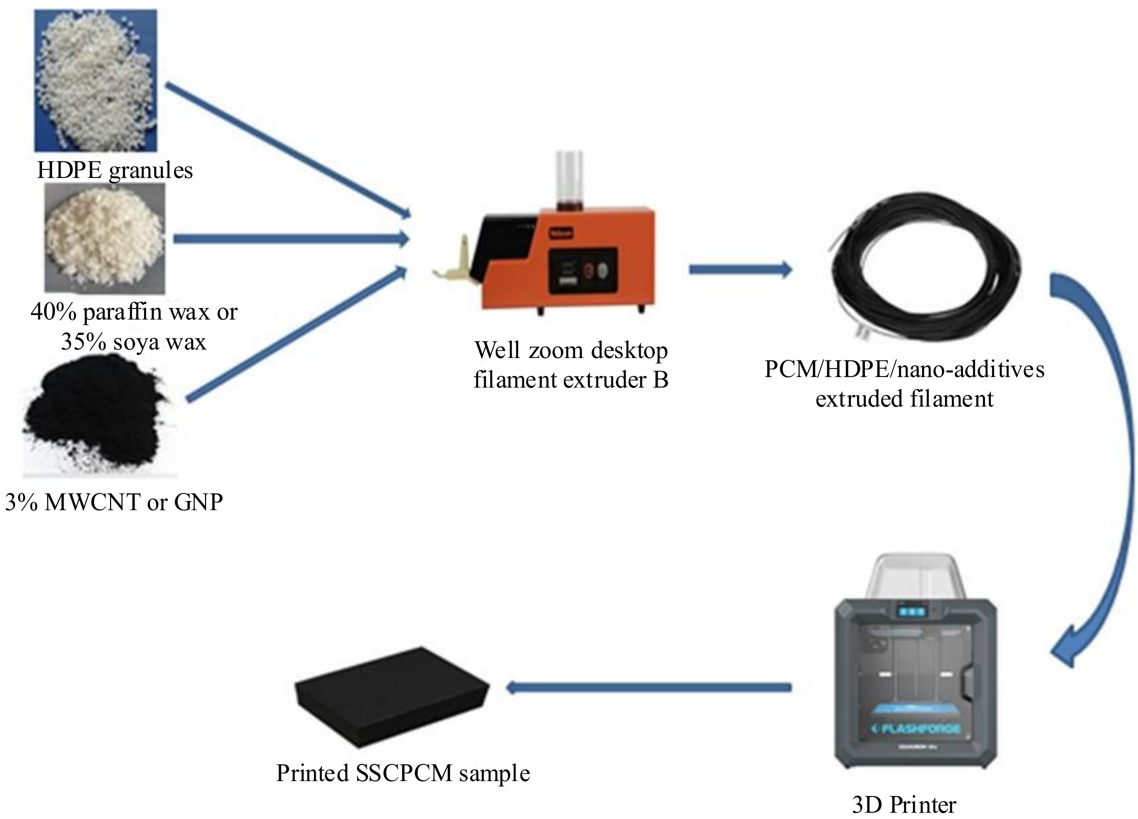


**Figure 2.** Samples of 3-D printed SSCPCM are prepared schematically.

 

### Preparation of 3d-Printed SSCPCM Samples

The SSCPCM samples were 3D printed using an Ultimaker 3 Extended printer. This printer utilizes Fused Deposition Modeling (FDM) technology. For G-code generation, Ultimaker Cura software was employed. Figure 3 Depicts the Ultimaker 3 Extended printer used for fabrication. A heated HDPE build plate set at 60 °C provided strong adhesion, reducing curling and delamination, which were brought on by the temperature differential between the ambient environment (25 °C) and the extruded material (235 °C). By visually screening the filament before use and modifying the material rate of flow, printing issues like nozzle obstructions, under-extrusion from inconsistent filaments, and PCM leakage at elevated enclosure temperatures above 42 °C were lessened. Extruder clogs were also reduced by lowering the print speed. Table 2 lists printer parameters used during fabrication of SSCPCM samples via FDM.

To improve interlayer bonding and reduce defects, a controlled heated environment at 60–65 °C was implemented, significantly enhancing print quality. Initial adhesion issues resulted in difficulties when removing the prints from the build plate, leading to a design modification where additional depth was added to the samples. Figure 2 shows the schematic preparation of 3D printed SSCPCM samples. When necessary, the final surface was sanded to achieve the desired finish and 40mmx40mmx10mm four square plates were successfully prepared. Figure 4 shows images of 3D printed SSCPCM samples with dimensions (40 mm × 40 mm × 10 mm)

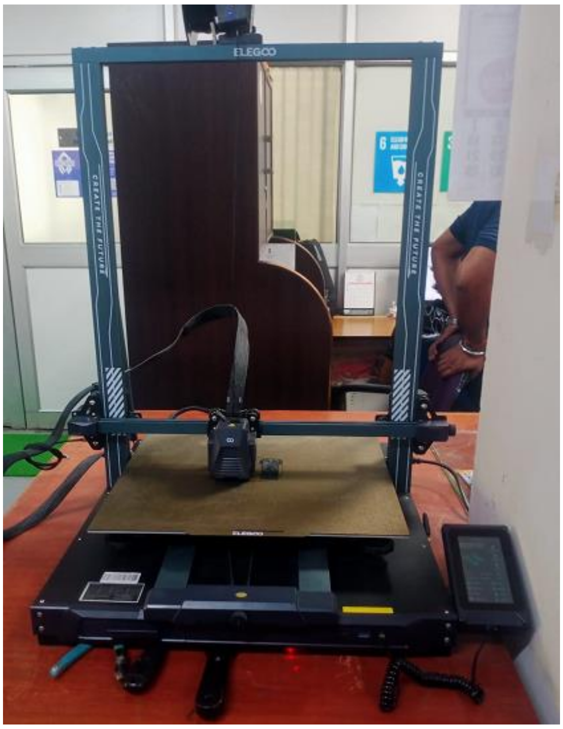


**Figure 3.** 3D Printer (Fused Filament Fabrication).

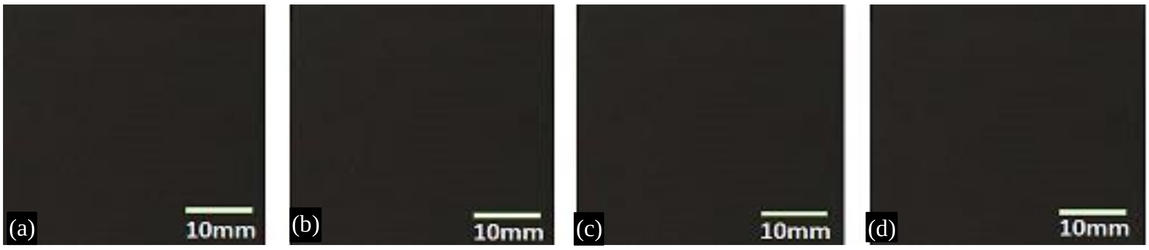


**Figure 4.** Images of 3D printed SSCPCM samples with dimensions (40 mm × 40 mm × 10 mm) (a)HDPE/PW/MWCNT3 (b) HDPE/PW/GNP3 (c) HDPE/SW/MWCNT3 (d) HDPE/PW/GNP3.

 

**Preparation of Molded SSCPCM Samples**

Utilizing the same material as above that were 3D printed. First, HDPE was melted for 15 minutes at 110 °C on a hot plate. After that, liquid paraffin or soy wax was poured and combined with the melted HDPE for a further fifteen minutes. After that, a magnetic stirrer was used to agitate the composite mixture for 15 minutes at 800 rpm while keeping the temperature at 70 °C. This was followed by 15 minutes of ultrasonication at 20 kHz to improve dispersion. To guarantee even dispersion of the components, the composite was then manually mixed for 30 minutes at 110 °C on a hot plate. The molded SSCPCM samples were then created by pouring the liquid composite into a mold and letting it cool at ambient temperature for half an hour [16]. Figure 5 Similar to Figure 4, but showing molded rather than 3D-printed samples.

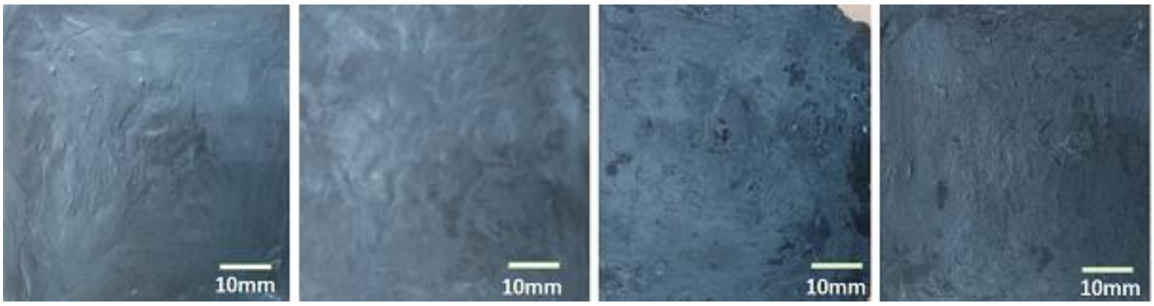


**Figure 5.** Images of molded SSCPCM samples with dimensions (40 mm × 40 mm × 10 mm) (a) HDPE/PW/MWCNT3 (b) HDPE/PW/GNP3 (c) HDPE/SW/MWCNT3 (d) HDPE/PW/GNP3.

## RESULTS

### Thermal Storage

DSC (Perkin Elmer STA 8000) was used to determine the latent heat of fusion and transition temperature of SSCPCM/HDPE composite samples that were molded and 3D printed. Samples (6–18 mg) that had been molded and 3D printed were put in 40 µl aluminum crucibles and heated to 200 °C at a rate of 2 °C per minute. Heat flow was monitored every second. The onset and endset temperatures from the heat flow vs. temperature graph are used to establish the temperature range across which the phase shift of SSCPCM occurs because it is not a pure material. The area under the heat flow curve was used to determine the latent heat of fusion. The melting and freezing enthalpies of SSCPCM/PW and SSCPCM/SW were 93.6 J/g and 86.9 J/g, respectively. Due to the lower weight percentage of PW and SW in SSCPCM, the inclusion of nano-additives (GNP and MWCNT) somewhat decreased enthalpy while maintaining high thermal energy storage efficiency. The enthalpy decrease increases with the additive proportion. Additionally, nano-additives improved heat transfer rates, leading to earlier melting in HDPE/PW/GNP3, HDPE/PW/MWCNT3, HDPE/SW/GNP3, and HDPE/SW/MWCNT3 compared to HDPE/PW and HDPE/SW. Table 3 Provides melting/freezing temperatures and enthalpy values for both types of samples.While 3D-printed SSCPCM samples showed improved thermal conductivity due to enhanced interfacial bonding and better dispersion of nano-additives, both molded and 3D-printed samples exhibited similar latent heat storage behavior, indicating that the phase-change characteristics remained largely unaffected by the fabrication method. Figure 6 Displays the heat flow vs. temperature curves used to derive melting/freezing data and enthalpies of the samples.

### Thermal Conductivity

The ability of a substance to conduct heat is measured by its thermal conductivity, which plays a crucial role in determining its suitability for thermal management applications. was evaluated using the TPS technique, a spiral-shaped nickel sensor, sandwiched between Kapton layers, was applied to all SSCPCM samples. Each sample underwent three tests to confirm accuracy, and the average measurement was recorded. Since PCMs generally exhibit low thermal conductivity, nano-additives such as MWCNT and GNP were incorporated to enhance heat transfer while maintaining the PCM's chemical integrity. Among the molded samples, the highest thermal conductivity values recorded were 0.86 W/m-K for HDPE/SW/GNP3 (218.5% increase), 0.84 W/m-K for HDPE/SW/MWCNT3 (211.1% increase), 0.72 W/m-K for HDPE/PW/GNP3 (213.0% increase) and 0.83 W/m-K for HDPE/PW/MWCNT3 (260.8% increase). Due to improved dispersion of nano-additives in the matrix and improved interfacial bonding, an extra 10–15% increase in heat conductivity was noted when the same compositions were 3D printed. Figure 7 Graphically represents thermal conductivity differences between molded and 3D-printed SSCPCM samples. HDPE/SW/GNP3, HDPE/SW/MWCNT3, HDPE/PW/GNP3 and HDPE/PW/MWCNT3 all had increases in thermal conductivity of 0.95 W/m-K (10.5%), 0.93 W/m-K (9.7%),.87W/m-K (20.9%) and 0.91 W/m-K (9.6%) after 3D printing. Table 4 highlights improvements in thermal conductivity for 3D-printed samples vs. molded.

**Table 3.** Thermal Energy Storage Parameters of Molded and 3D Printed SSCPM Samples.

| Sample type | Sample ID | Melting point (ºC) | Freezing point (ºC) | Melting enthalpy(J/g) | Freezing enthalpy (J/g) |
|---|---|---|---|---|---|
| Molded Sample | HDPE/PW/MWCNT3 | 42.7 | 54.6 | 80.4 | 74.7 |
| 3D Printed Sample | HDPE/PW/ MWCNT3 | 42.3 | 54.4 | 82.1 | 75.2 |
| Molded Sample | HDPE/SW/ MWCNT3 | 44.6 | 57.2 | 74.2 | 70.6 |
| 3D Printed Sample | HDPE/SW/ MWCNT3 | 44.4 | 57.3 | 74.3 | 70.4 |
| Molded Sample | HDPE/PW/GNP3 | 42.3 | 52.5 | 82.1 | 76.8 |
| 3D Printed Sample | HDPE/PW/ GNP3 | 42.3 | 52.2 | 82.2 | 76.6 |
| Molded Sample | HDPE/SW/ GNP3 | 44.8 | 57.4 | 75.3 | 70.2 |
| 3D Printed Sample | HDPE/SW/ GNP3 | 44.9 | 57.3 | 75.4 | 70.4 |

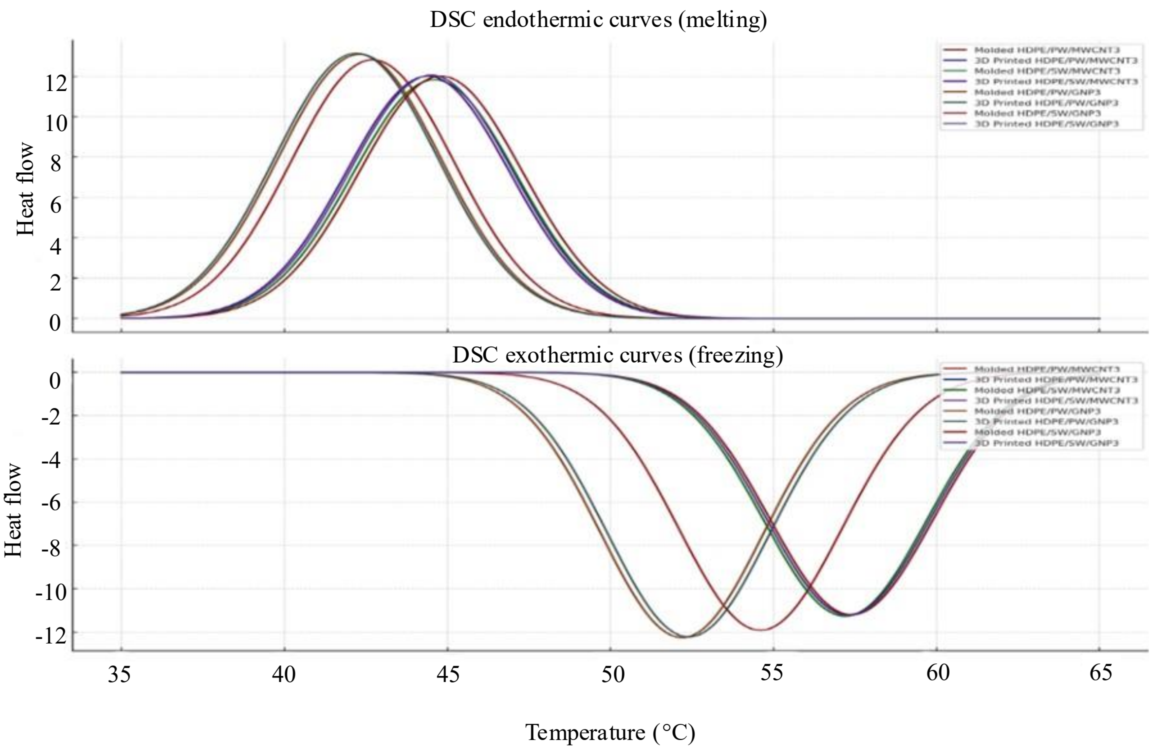


**Figure 6.** DSC thermographs.

ISSN: 2321-2810 (Online), ISSN: 2321-8525 (Print)

**Table 4.** Comparison of Molded and 3D-Printed SSCPCM Samples.

| Sample | Molded thermal conductivity (W/m-K) | % Increase (compared to base PCM) | 3D-printed thermal conductivity (W/m-K) | % Increase (compared to molded) |
|---|---|---|---|---|
| HDPE/SW/GNP3 | 0.86 | 218.5% | 0.95 | 10.5% |
| HDPE/SW/MWCNT3 | 0.84 | 211.1% | 0.93 | 9.7% |
| HDPE/PW/GNP3 | 0.72 | 213.0% | 0.87 | 20.9% |
| HDPE/PW/MWCNT3 | 0.83 | 260.8% | 0.91 | 9.6% |

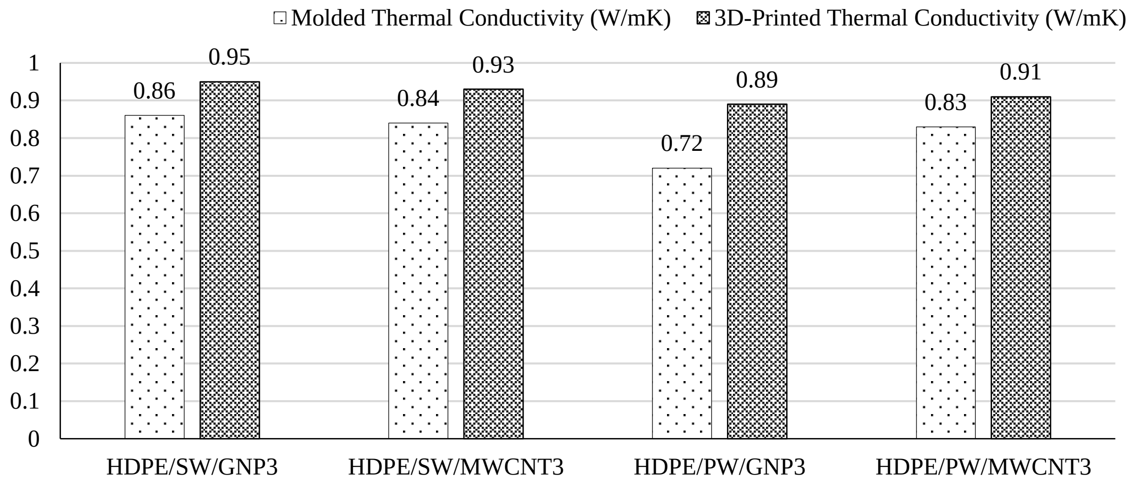


**Figure 7.** Comparative analysis of molded and 3D printed samples.

## CONCLUSIONS

In conclusion, the study demonstrated the successful fabrication of both molded and 3D-printed shape-stabilized PCM (SSCPCM) composites using HDPE, paraffin wax, soya wax, and nano-additives (MWCNT and GNP). The DSC analysis confirmed that both molded and 3D-printed samples exhibited similar latent heat storage behavior, with melting and freezing enthalpies of 93.6 J/g and 86.9 J/g, respectively, despite slight reductions due to nano-additive incorporation. However, the inclusion of nano-additives significantly enhanced thermal conductivity, with molded samples showing improvements of over 200%, and 3D-printed samples further increasing conductivity by 10–15% due to improved interfacial bonding and dispersion. The successful 3D printing of SSCPCM samples, despite challenges such as nozzle clogging and adhesion issues, highlights the feasibility of uses of additive manufacturing for thermal energy storage. According to the results, 3D printing may be a useful method for creating high-performance SSCPCM materials with exceptional thermal characteristics, which would make them appropriate for cutting-edge energy storage and thermal management applications.

## RECOMMENDATION FOR FUTURE WORK

For future work, further optimization of the 3D printing process parameters, including print speed, extrusion temperature, and layer thickness, could enhance the structural integrity and thermal performance of SSCPCM composites. Investigating alternative polymer matrices with higher thermal conductivity or flexibility may improve mechanical stability and thermal efficiency. Additionally, exploring hybrid nano-additives or surface-functionalized nanoparticles could further enhance heat transfer while minimizing the reduction in latent heat storage. Long-term thermal cycling studies should be conducted to assess the durability and reliability of 3D-printed SSCPCMs under real-world conditions. Finally, integrating these composites into practical energy storage systems, such as building envelopes or thermal management devices, could validate their performance and facilitate large-scale implementation in sustainable energy applications.

**REFERENCES**


1. Moon, H., Miljkovic, N., and King, W. P., "High power density thermal energy storage using additively manufactured heat exchangers and phase change material," International Journal of Heat and Mass Transfer, Vol. 153, 2020, p. 119591. https://doi.org/10.1016/j.
2. Ma, J., Ma, T., Cheng, J., and Zhang, J., "Polymer Encapsulation Strategy toward 3D Printable, Sustainable, and Reliable Form-Stable Phase Change Materials for Advanced Thermal Energy Storage," ACS Applied Materials & Interfaces, Vol. 14, No. 3, 2022, pp. 4251–4264. https://doi.org/10.1016/j.ijheatmasstransfer.2020.119591
3. Nofal, M., Pan, Y., and Al-Hallaj, S., "Selective Laser Sintering of Phase Change Materials for Thermal Energy Storage Applications," Procedia Manufacturing, Vol. 10, 2017, pp. 851–865. https://doi.org/10.1016/j.promfg.2017. 07.071
4. Nofal, M., Al-Hallaj, S., and Pan, Y., "Experimental investigation of phase change materials fabricated using selective laser sintering additive manufacturing," Journal of Manufacturing Processes, Vol. 44, 2019, pp. 91–101. https://doi.org/10.1016/j.jmapro.2019.05.043
5. Wei, P., Cipriani, C. E., and Pentzer, E. B., "Thermal energy regulation with 3D printed polymer-phase change material composites," Matter, Vol. 4, No. 6, 2021, pp. 1975–1989. https://doi.org/10.1016/j.matt.2021.03.019
6. Zhang, Y., Ma, G., Wang, J., Liu, S., and Kang, S., "Numerical and experimental study of phase-change temperature controller containing graded cellular material fabricated by additive manufacturing," Applied Thermal Engineering, Vol. 150, 2019, pp. 1297–1305. https://doi.org/10.1016/j. applthermaleng.2019.01.066
7. Cao, M., Huang, J., and Liu, Z., "The Enhanced Performance of Phase Change Materials via 3D Printing with Prickly Aluminum Honeycomb for Thermal Management of Ternary Lithium Batteries," Advances in Materi als Science and Engineering, Vol. 2020, 2020, pp. 1–11. https://doi.org/10. 1155/2020/8167386
8. Hirano, S., and Kawanami, T., "Thermal Characteristics and Development of a Phase Change Material for Thermal Energy Storage Media as Thermo Functional Fluids," Tetsu-to-Hagane, Vol. 106, No. 8, 2020, pp. 581–590. https://doi.org/10.2355/tetsutohagane.TETSU-2019-127
9. Tamraparni, A., Hoe, A., Deckard, M., Zhang, C., Elwany, A., Shamberger, P. J., and Felts, J. R., "Experimental Validation of Composite Phase Change Material Optimized for Thermal Energy Storage," 2021 20th IEEE Interso ciety Conference on Thermal and Thermomechanical Phenomena in Electronic Systems (iTherm), IEEE, San Diego, CA, USA, 2021, pp. 551–555. https://doi.org/10.1109/ITherm51669.2021.9503204
10. Guo, Y., Yang, H., Fu, W., Bai, L., and Miao, J., "Temperature contr ol of star sensor baffle using 3D printing and PCM thermal energy storage technology," International Journal of Heat and Mass Transfer, Vol. 165, 2021, p. 120644. https://doi.org/10.1016/j.ijheatmasstransfer.2020.120644
11. Zhu, C.; Hao, Y.; Wu, H.; Chen, M.; Quan, B.; Liu, S.; Hu, X.; Liu, S.; Ji, Q.; Lu, X.; et al. Self-Assembly of Binderless MXene Aerogel for Multiple-Scenario and Responsive Phase Change Composites with Ultrahigh Thermal Energy Storage Density and Exceptional. Electromagnetic interference shielding Nonomicro Lett.2024, 16, 52 https://doi.org/10.1007/s40820-024-01582-3
12. Wang, C., and Liu, C., "Additive Manufacturing of Shape-Stabilized Compos ite Phase Change Materials Via Ultraviolet Curing," SSRN Electronic Jour nal, 2022. https://doi.org/10.2139/ssrn.4173655
13. Yang, W., Zhou, F., Chen, X., and Zhang, Y., "Performance analysis of axial air cooling system with shark-skin bionic structure containing phase change material," Energy Conversion and Management, Vol. 250, 2021, p. 114921. https://doi.org/10.1016/j.enconman.2021.114921
14. Yazdani, M. R., Laitinen, A., Helaakoski, V., Farnas, L. K., Kukko, K., Saari, K., and Vuorinen, V., "Efficient storage and recovery of waste heat by phase change material embedded within additively manufactured grid heat exchangers," International Journal of Heat and Mass Transfer, Vol. 181, 2021, p. 121846. https://doi.org/10.1016/j.ijheatmasstransfer.2021.121846
15. Qu, Y.; Wang, S.; Tian, Y.; Zhou, D. Comprehensive evaluation of Paraffin-HDPE shape stabilized PCM with hybrid carbon nano-additives. *Appl. Therm. Eng.* 2019, *163*, 114404. https://doi.org/10.1016/j.applthermaleng.2019.114404


 

16. Yadav, D.K., Rathore, P.K.S., Singh, R.K., Gupta, A.K. and Sikarwar, B.S., 2024. Experimental Study on Paraffin Wax and Soya Wax Supported by High-Density Polyethylene and Loaded with Nano-Additives for Thermal Energy Storage. *Energies* https://doi.org/10.3390/en17112461
17. Palanisamy, S., Karuppiah, G., Kumar, P., Dharmalingam, S., Mubarak, S., Santulli, C., Ayrilmis, N. and Karumuri, S., 2024. Effect of Process Parameters and Material Selection on the Quality of 3D Printed Products by Fused Deposition Modeling (FDM): A Review. *Advances in Polymer Technology*, *2024*(1), p.3480281. https://doi.org/10.1155/adv/3480281
18. Kechagias, J.D., Ninikas, K., Vakouftsi, F. *et al.* Optimization of laser beam parameters during processing of ASA 3D-printed plates. *Int J Adv Manuf Technol* 130, 527–539 (2024). https://doi.org/10.1007/s00170-023-12711-4
19. Ayrilmis, N., Yurttas, E., Avsar, E. Y., Kahraman, M. V., Özdemir, F., Palanisamy, S., Yetiş, F., Ali, S. K., Gurusamy, M. K., Palaniappan, M., and Al-Farraj, S. A. (2025). "Properties of plastic composites filled with giant reed flour and magnesium oxide nanoparticles," *BioResources* 20(2), 2670–2686. https://doi.org/10.15376/biores.20.2.2670-2686
20. Mubarak, S., Byun, H.S., Dhamodharan, D., Divakaran, N., Kumar, P.A., Siddique, A.B., Wang, J., Kumar, M.P., Mangalaraja, R.V. and Palanisamy, S., 2024. Functionalized black phosphorous-based polymer nanocomposites. In *Advances in Functionalized Polymer Nanocomposites* (pp. 307-337). Woodhead Publishing. https://doi.org/10.1016/B978-0-443-18860-2.00016-5

 